water

MDPI

Article

Evaluation of a Smectite Adsorption-Based Electrostatic System to Decontaminate F^- Rich Thermal Waters

Fabio Fanari [1], Matteo Bruno Lodi [2], Worash Getaneh [3], Alessandro Fanti [2], Francesco Desogus [1,*] and Paolo Valera [4,5]

[1] Department of Mechanical, Chemical and Material Engineering, University of Cagliari, 09123 Cagliari, Italy; f.fanari@dimcm.unica.it
[2] Department of Electrical and Electronic Engineering, University of Cagliari, 09123 Cagliari, Italy; matteobrunolodi@ieee.org (M.B.L.); alessandro.fanti@diee.unica.it (A.F.)
[3] School of Earth Sciences, Addis Ababa University, Addis Ababa 1176, Ethiopia; worash.getaneh@aau.edu.et
[4] Department of Civil and Environment Engineering and Architecture, University of Cagliari, 09123 Cagliari, Italy; pvalera@unica.it
[5] Institute of Environmental Geology and Geoengineering, National Research Council, 09123 Cagliari, Italy
* Correspondence: f.desogus@dimcm.unica.it

Abstract: Several studies have shown the presence of fluoride levels much higher than the 1.5 mg/L threshold concentration recommended by WHO in the spring waters and wells of the Ethiopian Rift Valley. Available defluoridation techniques can be costly, present complicated technical aspects, and show limited effectiveness. Therefore, it is necessary to devise innovative, sustainable, and effective solutions. This study proposes an alternative method of intervention to the known techniques for removing fluoride from water, particularly suitable for smaller rural communities. In particular, in this work, the possibility to use electromagnetic fields as a physical method for removing the excess fluoride was investigated. The study was carried out by developing a multiphysics model used for studying and envisaging the design of a device. In this framework, the combination of this approach with the use of highly reactive smectite clay was numerically studied. The results obtained, although preliminary, indicate that the proposed system could significantly impoverish the waters of the Rift Valley from fluoride, with the consequence of obtaining a resource suitable for human consumption, in particular for rural communities. However, further theoretical investigations and experimental phases will be necessary to achieve the desired results.

Keywords: adsorption; electric field; Ethiopian Rift Valley; fluoride; fresh water; Langmuir isotherm; smectite clay; thermal water

Citation: Fanari, F.; Lodi, M.B.; Getaneh, W.; Fanti, A.; Desogus, F.; Valera, P. Evaluation of a Smectite Adsorption-Based Electrostatic System to Decontaminate F^- Rich Thermal Waters. *Water* **2022**, *14*, 167. https://doi.org/10.3390/w14020167

Academic Editor: Laura Bulgariu

Received: 7 December 2021
Accepted: 6 January 2022
Published: 8 January 2022

1. Introduction

A recent WHO report [1] shows that one in three people in the world do not have access to safe drinking water, with a particularly high percentage in rural areas. Furthermore, many studies and research, and the consequent actions carried out so far, have been mainly aimed at accessibility to water for human consumption, but the experience of the pandemic has brought a very important lesson, namely the monetary and social costs that non-accessibility entails. In fact, we want to emphasize how much globalization has now linked populations around the world, and the COVID-19 pandemic is a very effective example of this. As described in the joint UNICEF–WHO report [2], we are now beginning to understand how important access to clean water is, not only for consumption (food and irrigation) but also for hygiene, i.e., a type of use which has proved to be fundamental to countering the pandemic. This will lead to a foreseeable significant increase in water demand compared to the parameters considered up to now. The above highlights the importance of having data and information available on the various types of existing aquifers in the various territories, their characteristics, and, finally, the protocols to be

applied both for their exploitation and for safeguarding the resource. Based on these considerations, research aimed at studying new water treatment methods that are simple and that do not require advanced technologies or materials for their operation is therefore essential to allow a wider and more targeted use. The model proposed here has the purpose of depleting the fluorine from water, providing the possibility of an efficient use for other elements which are potentially harmful to human health (As, Cd, etc.) and that are present in ionic form. Fluorosis is endemic to approximately twenty developing and developed nations. India, China, and African countries of the Rift Valley region are the most severely affected [3].

The starting hypothesis of this work is based on the significant fluorine content of the geothermal springs present in the area of the Ethiopian Rift Valley; this content is in ionic form and these springs have an upward thrust which is sometimes considerable [4–8]. This suggests that, thanks to the Hall and Faraday effects, the ions dispersed in the hydrothermal water can be seized through magnetic or electric fields, at medium-high enthalpy, towards natural traps consisting of smectite clay, easily available in situ [9], in the tertiary volcanites, which make up most of the rocks outcropping in the Rift Valley border [8]. A sample of soil, collected in the tertiary basaltic lavas of the Muger region, with evident alteration, is the one that presented the best performance in the absorption of fluoride [9]. The parent rocks for the smectite-rich soils are scoriaceous basalts which produced the soil through surface alterations. The analysis of this sample [9] made it possible to identify, through X-ray powder diffraction (XRPD) analysis, the minerals present, mainly pyrophyllite, plagioclase, and smectite. Smectites are a group of phyllosilicate mineral species represented mainly by montmorillonite, beidellite, nontronite, saponite, and hectorite. Smectites are types of clay minerals that are common in soils developed in temperate regions. Soils rich in smectite are considered to be very effective at attenuating many organic and inorganic pollutants because of the high surface area and adsorptive properties of the smectites [10]. They adsorb anions by three different mechanisms: by electrostatic interaction with particle edges when these are positively charged [11,12], by exchanging structural OH groups at the edges and also on basal (planar) surfaces (e.g., [13]), and by accompanying multivalent cations at exchange positions [14].

The smectite clay available in these lithologies should not present particular difficulties to the exploitation. Conversely, zeolites, present in the pyroclastic rocks of the Rift Valley, have very high values of fluorine reaching the saturation of the zeolites themselves, and therefore cannot be taken into consideration for use in the system.

In the literature, several methods for fluoride removal from water are reported: coagulation and precipitation [15], adsorption [16], nanofiltration [17], reverse osmosis [18], membrane-based [19], electrodialysis [20], and crystallization [21]. Among these methods, with regard to defluoridation for obtaining drinking water, adsorption is one of the most suitable due to its low operational costs, relative ease of use, and its capacity to produce water of an excellent quality since it does not contaminate it with other undesirable components or generating sludges [22]. Several adsorbents have been tested for water defluoridation. These include graphene and carbon-based materials [23,24], modified alumina [25,26], porous MgO nanostructures [27], zeolites [28,29], Ce–Zn ceramic oxides [30], and even bio-based materials [31,32]. However, the combination of adsorption methods and physical fluoride removal strategies based on static electric fields has been poorly investigated. This work deals with the in silico investigation of a novel solution to impoverish fluoride-rich thermal waters. The proposed system allows modulating the various depletion stages, which could vary with varying conditions, in order to obtain the maximum efficiency in the removal of fluoride. In this paper, we describe a theoretical model for the removal of fluorine, coupling an electric field and adsorption on smectite clay to demonstrate the synergy between them. Furthermore, the designed system is modular, allowing a specific amount of water to be treated depending on the needs of a single rural community.

2. Materials and Methods

2.1. System Configuration

The simulated device consists of a parallelepiped-shaped container with two stainless steel plates facing each other and in contact with the outer surfaces of the device, i.e., not in contact with the aqueous medium. A constant voltage V_0 is applied to these plates; thus, they act as external electrodes with the same voltage, but with a sign opposite to each other (V− and V+ in Figure 1). The length of these plates is equal to the length of the container (L, in Figure 1), while their distance (equal to the container width, $w = w_w + w_s$) was varied during the study to analyze the fluoride removal process as a function of the distance between the electrodes, and so of the mass of water to treat, in relationship with a constant amount of adsorbent material in the system. The height of the container was not taken into account for symmetry reasons, using a 2D physics simulation of the system. Therefore, the results can be considered normalized for the unit of height. The container is filled with water for a width w_w (Figure 1) and a layer of mineral (smectite clay) powder of a fixed thickness (w_s, Figure 1), divided by a permeable septum. Fluoride in water was simulated as released by the dissolution of a salt, and NaF was chosen for the scope. The fluoride anions (F^-, in Figure 1) present in the water are attracted by the positively charged plate, whereas the sodium cations (Na^+, in Figure 1) move to the negatively charged surface. The mineral layer is positioned adjacent to the container surface where the positively charged plate is positioned, in order to enhance the motion of the F^- towards the adsorbent material. A schematic representation of the simulated device is reported in Figure 1.

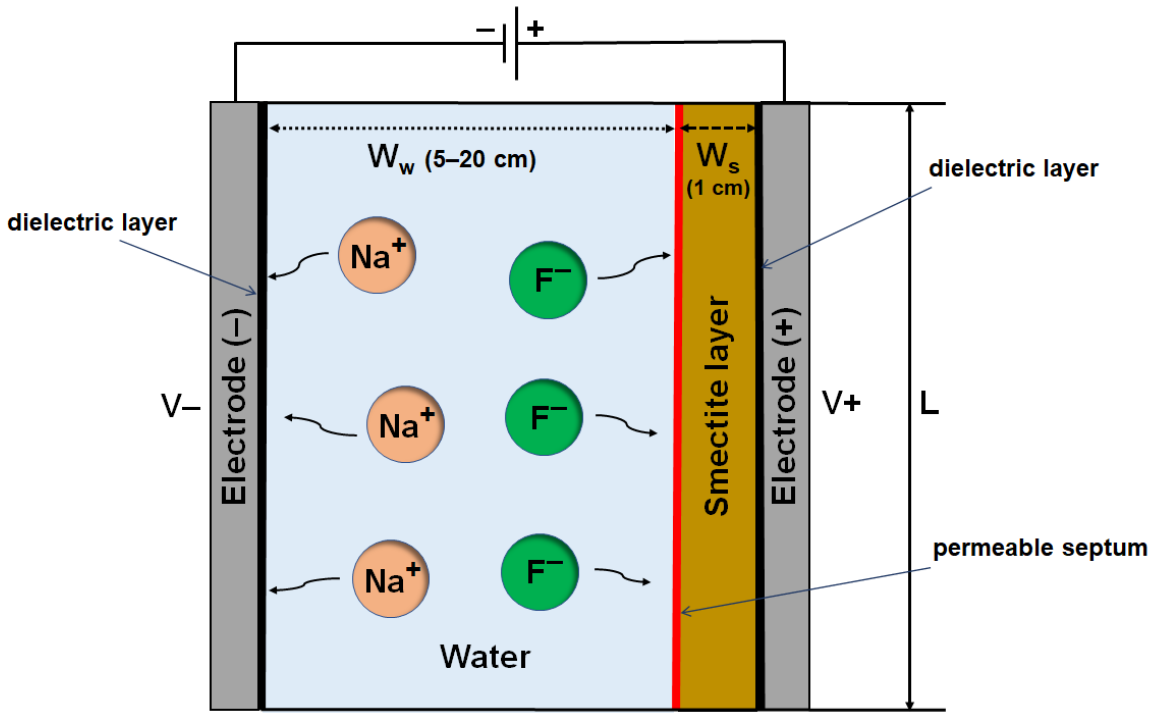

Figure 1. Top view schematic representation of the simulated device.

2.2. Mathematical Modeling and Equations

The ions motion mechanisms which are involved in the system are (i) the diffusion in the water and (ii) the migration induced by the electric field. Once the F^- anions reach the mineral layer, they first externally diffuse to the particles, then diffuse into the latter, and finally, they are adsorbed on the mineral surface. In the literature, the migration dynamic of an ion population to a charged surface, at which an electrostatic potential V_0 is applied, is typically given in terms of the dilute solution theory [33–40]. Provided that, with respect to the thermal energy, the potential is small enough, under this well-

known approximation, the ions' concentration fields are supposed to follow a Boltzmann's distribution (Equation (1)) [41]:

$$c_i = c_{i_0} e^{-zeV_0/k_B T}, \quad (1)$$

where C_{i_0} is the initial concentration of the i-th ion, z is the ion valence, e is the electron charge (C), k_B is the Boltzmann constant (J × K^{-1}), and T is the system temperature (in K). For values of voltage much higher than the thermal voltage ($V_t = k_B T/ze$), Equation (1) predicts an ionic concentration that exponentially blows up. As a consequence, the correspondent spatial charge distribution at the charged surface does not respect the physical limit due to the finite ion size, thus violating any steric principle. Therefore, in the literature, several models to modify the Poisson–Boltzmann (PB) equation have been proposed to deal with this problem. One of these models, which uses the mean-field approximation and works for low ion concentrations, was proposed by Kilic et al. [34]. The modified Poisson–Boltzmann (MPB) equation is as follows (Equation (2)):

$$\nabla^2 V_0 = \frac{zec_{i0}}{\varepsilon} \frac{2sinh\left(\frac{zeV}{k_B T}\right)}{1 + 2v\, sinh^2\left(\frac{zeV}{2k_B T}\right)}, \quad (2)$$

where ε is the dielectric permittivity of the solution, V is the electrostatic potential in volts, and v is a factor of non-diluteness, which accounts for the steric and volume effects, defined as follows [34,35]:

$$v = 2a^3 c_{i0}, \quad (3)$$

where a is the typical spacing between densely packed ions, reached at a critical potential V_c, that is no more than a few times V_t. This modification of the model was to ensure that the system can saturate to a maximum concentration value of counterions packed with typical spacing a near a highly charged surface equal to $C_{imax} = a^{-3}$ [42]. Thus, the amount of charge attracted to the charged surfaces cannot be infinite, avoiding the electrostatic potential to blow up locally, i.e., an effective, but finite, charge density distribution can be found from Equation (2).

Within the MPB model, the spatio-temporal migration dynamics of i-th ionic populations (therein F^- and Na^+) in the system can be studied by writing the macroscopic mass transport balances, which can be modeled through the following nonlinear electro migration–diffusion equations [35]:

$$\frac{\delta c_n}{\delta t} = D_n \nabla^2 c_n + \frac{D_n}{k_B\, T}\, ze\, \nabla\cdot(c_n \nabla V) + a^3 D_n \nabla\cdot\left(\frac{c_n \nabla\left(c_p + c_n\right)}{1 - c_p a^3 - c_n a^3}\right), \quad (4)$$

where D_n is the ion diffusion coefficient in water in m^2/s, c_p is the positive ion concentration, and c_n is the concentration of the negative ion (F^- in this case). It is also possible to define the ionic mobility μ using the Nernst–Einstein relationship [43]:

$$\mu_n = \frac{zeD_n}{k_B\, T} \quad (5)$$

The molar balance for F^- can be written following the mass continuity equation [44]:

$$\frac{\delta c_n}{\delta t} + \nabla\cdot J_n = 0, \quad (6)$$

where the flux J_n in the water can be defined using the Nernst–Planck equation [44]:

$$J_n = -D_n\, \nabla c_n - \mu_n\, F\, c_n \nabla V_0, \quad (7)$$

while in the porous media it can be written as

$$J_n = -(D_{Dn} + D_{en})\,\nabla c_n - \mu_n\,F\,c_n \nabla V_0, \tag{8}$$

where D_{Dn} is the coefficient of dispersion of the F^- in the porous material in m^2/s, F is the Faraday constant, and D_{en} is the effective diffusion coefficient in m^2/s. Based on the Millington and Quirk model [45], D_{en} can be defined as reported in Equation (9):

$$D_{en} = \frac{\epsilon_p}{\tau_{f_n}}\,D_n, \tag{9}$$

where ε_p is the porosity of the adsorbent material while τ_{f_n} is the tortuosity, defined as

$$\tau_{f_n} = {\epsilon_p}^{-1/3}, \tag{10}$$

The adsorption equilibrium in the mineral was modeled using the Langmuir adsorption model [46]:

$$C_{p_n} = \frac{K_{L_n} c_{pmax_n} c_n}{1 + K_{L_n} c_n}, \tag{11}$$

where c_n is the water concentration of F^- at equilibrium (mol/m^3), C_{p_n} is the amount of F^- adsorbed per unit mass of adsorbent (mol/kg), K_{L_n} is the constant related to the free energy of adsorption (m^3/mol), and c_{pmax_n} is the maximum adsorption capacity of the porous media (mol/kg), corresponding to the saturation limit.

2.3. Simulation Overview

The simulations were performed using the commercial FEM software COMSOL Multiphysics V5.5 (COMSOL, Inc., Burlington MA, USA). In particular, the MPB Equation (2) was solved using the Mathematics module coupled with Poisson's equation module while the drift-diffusion equation and adsorption in the porous media were implemented with the Transport of Diluted Species interface. The values of the parameters used for the simulation are reported in Table 1; some of these are derived from other works found in the literature and cited in column 4. The diffusion and dispersion coefficients of Na^+ and F^- were considered equal for the two ions ($D_n = D_p$, $D_{Dn} = D_{Dp}$) and constant, neglecting the effects of the ion concentrations and local differences in temperature that in this case are not significant and can be neglected [42]. Regarding V_0, this was varied between 0 and 9 V with variable steps in order to study the effect of the applied electrostatic potential. Another parameter that was changed was the initial concentration of F^- in water for which two values were taken into account, 5 mg/L and 10 mg/L, according to the mean concentrations of the F^- rich water to treat, as reported in the Introduction section. Additionally, the width of the device layer containing water was varied, keeping the mineral layer width constant to analyze the efficiency of the system in the defluoridation of higher volumes of water.

The time useful to reduce the concentration to the limit of 1.5 mg/L was calculated using the function "levelcrossing" of Origin (v.9.0 PRO, OriginLab Corporation, USA).

Table 1. Summary of the parameters used for the simulation setup.

Parameter	Description	Value	Reference
T	Temperature of the solution	37 °C	
ε	Dielectric constant of the solution	78	[42]
a	Spacing between densely packed ions	0.35 nm	[34,35]
D_n	F^- diffusion coefficient in water	1.35×10^{-9} m^2/s	[47]

Table 1. *Cont.*

Parameter	Description	Value	Reference
ϵ_p	Smectite clay layer porosity	0.33	[9]
ρ_p	Smectite clay layer density	1590 kg/m^3	[9]
D_{Dn}	Coefficient of dispersion of F^- in the porous material	7×10^{-10} m^2/s	[9]
K_{Ln}	Langmuir free energy adsorption constant	4.5391 m^3/mol	[9]
c_{pmaxn}	Langmuir maximum adsorption capacity	0.01476 mol/kg	[9]
V_0	Applied electrostatic potential	0–9 V	
L	Device length	1 m	
w_w	Water filled device width	5–20 cm	
w_s	Smectite filled device width	1 cm	
c_{n0}	Initial concentration of F^- in the water	5 mg/L; 10 mg/L	

3. Results

To understand the device working principles by some examples, in Figure 2 the fluoride concentration (c_{F^-}) profile along the system width for different times and applied voltages is reported. As can be seen from the first row of Figure 2, where the case of no applied voltage is presented, the only diffusion makes the ions move very slowly towards the mineral layer and the changes in the c_{F^-} profile are only due to adsorption. On the other side, looking at the second and the third rows of Figure 2, it is possible to observe, from the representation of the profile, that, applying raising voltages, the migration process is quicker and there is a faster decrease of c_{F^-} in the water.

This work aims to preliminarily demonstrate the feasibility of water defluoridation by an electric field aided adsorption-based system through the simulation of a device with the goal to reach a concentration of F^- in the water lower than 1.5 mg/L, the maximum threshold value suggested by WHO [48]. Taking into account this threshold, in Figure 3 the concentration distribution of F^- as a function of the handling time is reported for different values of V_0, c_{n0}, and w_w. The results are compared to the F^- threshold limit to show the defluoridation rate and time. The times required to reduce the fluoride concentration below the limit for each case study are reported in Table 2. At first, it is possible to appreciate that the only diffusion without the application of any voltage, even if useful and effective, is a very slow process, taking several days to reach the target concentration. On the other hand, the application of a voltage can strongly enhance the ions' migration [37], thus allowing them to be directed towards the positive pole and therefore towards the adsorbent material, smectite in our case. It can be noticed that the decrease in F^- with time becomes faster and faster when the applied voltage increases up to 9 V. Comparing the two different c_{n0} values analyzed, it is possible to state that, notwithstanding that a lower initial fluoride concentration requires a shorter defluoridation time, when V_0 increases, the differences in this treatment time fade away (see Table 2). Concerning the study of the device volume and of the ratio between the water to be treated and the mineral volumes, it can be noted that, as expected, by increasing the amount of fluorine-rich water, the defluoridation time also increases, but this detriment in the performance of the process can be easily compensated by increasing the applied voltage: for example, with w_w equal to 20 cm, instead of 5 cm, the volume of defluorized water considerably increases from 50 L/m to 200 L/m, and an applied voltage higher than 3 V, instead of 0.3 V, is necessary to perform the treatment in less than 1 day.

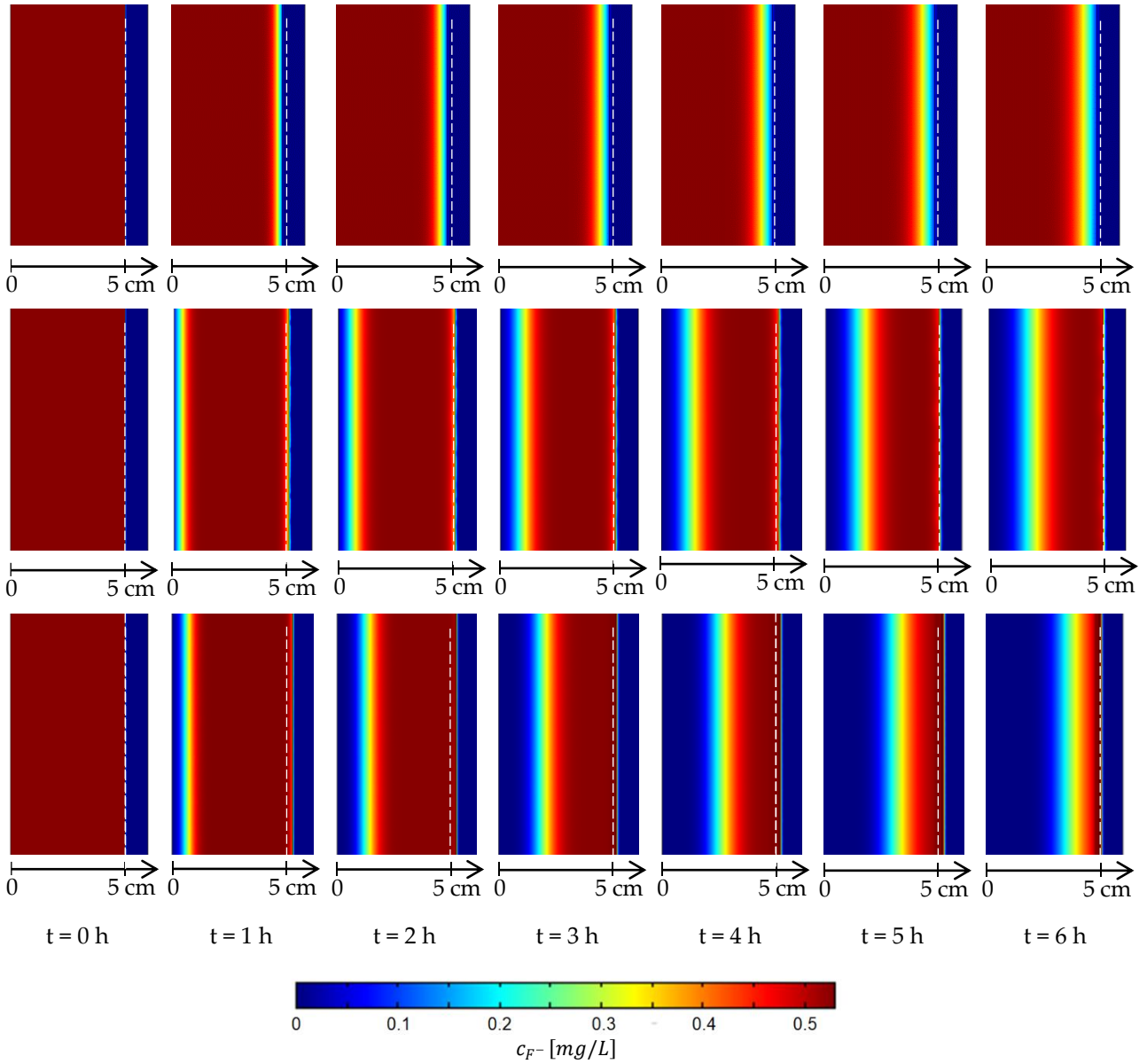

Figure 2. Fluoride concentration (mg/L) in the system as a function of time (t) for w_w = 5 cm and c_{n0} = 10 mg/L and applied voltage of 0 V (first row), 0.5 V (second row), and 1 V (third row).

Table 2. Time required to reduce the fluoride concentration below the limit of 1.5 mg/L as a function of applied voltage V_0, c_{no}, and w_w.

	Defluoridation Time (h)					
V_0	c_{n0} = 5 mg/L w_w = 5 cm	c_{n0} = 10 mg/L w_w = 5 cm	c_{n0} = 5 mg/L w_w = 10 cm	c_{n0} = 10 mg/L w_w = 10 cm	c_{n0} = 5 mg/L w_w = 20 cm	c_{n0} = 10 mg/L w_w = 20 cm
0 V	>48	>48	>48	>48	>48	>48
0.1 V	>48	>48	>48	>48	>48	>48
0.2 V	27.8	39.2	>48	>48	>48	>48
0.3 V	18.7	25.3	>48	>48	>48	>48
0.5 V	11.2	14.7	41.1	>48	>48	>48
1 V	5.6	7.1	20.6	26.0	>48	>48
3 V	1.9	2.3	6.9	8.5	26.3	32.5
5 V	1.1	1.4	4.1	5.1	15.8	19.5
9 V	0.6	0.8	2.3	2.8	8.8	10.8

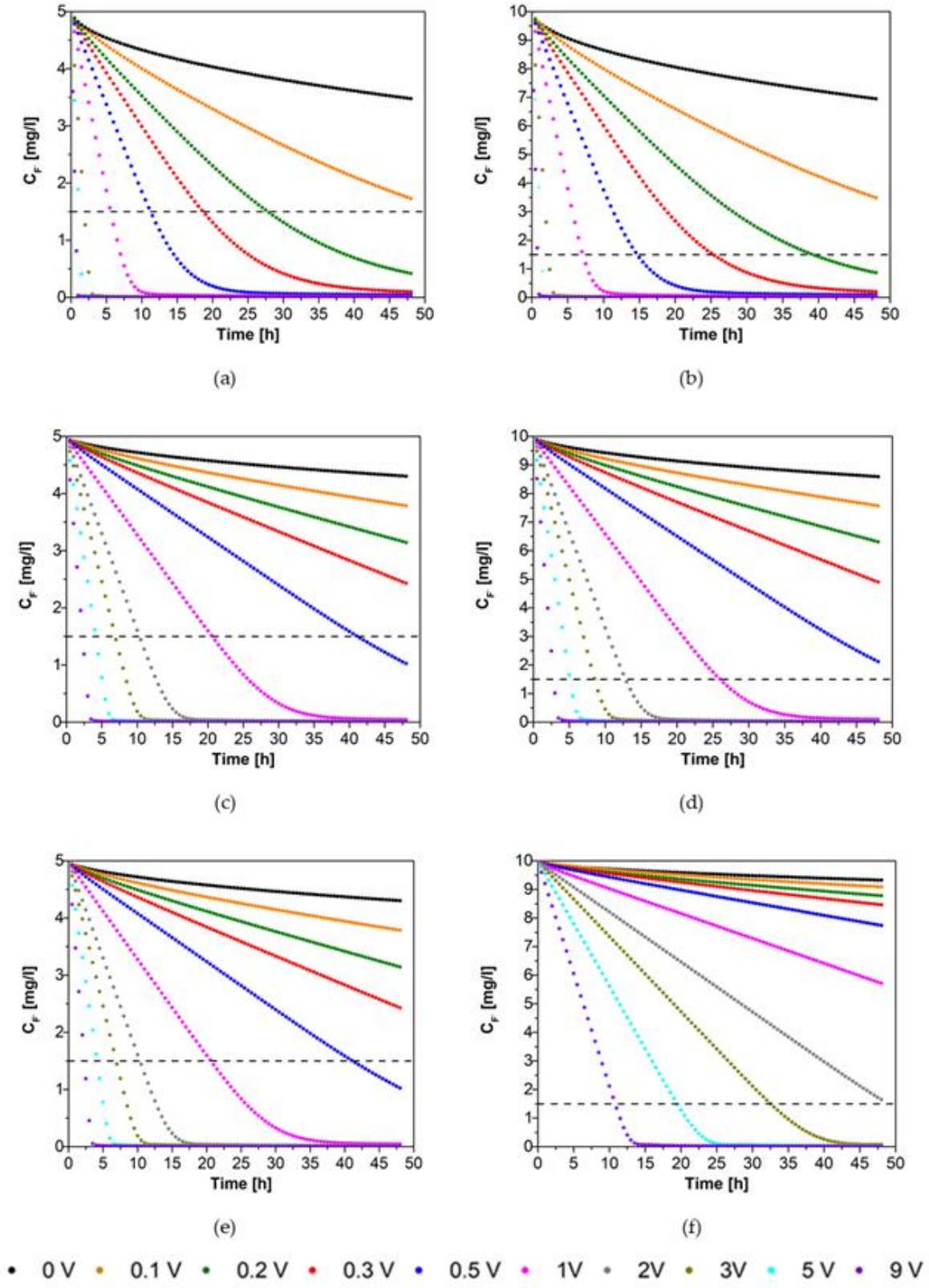

Figure 3. Fluoride concentration in water as a function of time and applied voltage V_0 for (**a**) $w_w = 5$ cm, $c_{n0} = 5$ mg/L; (**b**) $w_w = 5$ cm, $c_{n0} = 10$ mg/L; (**c**) $w_w = 10$ cm, $c_{n0} = 5$ mg/L; (**d**) $w_w = 10$ cm, $c_{n0} = 10$ mg/L; (**e**) $w_w = 20$ cm, $c_{n0} = 5$ mg/L; and (**f**) $w_w = 20$ cm; $c_{n0} = 10$ mg/L. The dashed line indicates the F^- threshold value discussed previously.

4. Discussion

This work aims to demonstrate the effectiveness of fluoride removal from drinking water, taking into account, as a case study, the applicability in the Ethiopian Rift Valley, where several springs with high concentrations of F^- ions are used daily for human consumption. This was done by considering a new technique based on the synergies between the adsorption capacity of local Ethiopian smectite clay and electromagnetic fields. As shown in the previous section, the smectites identified here present a good adsorption capacity at equilibrium; however, the deionization process would be very slow, due to the slow diffusion of ions in the static water, from the liquid bulk to the surface of the smectite solid particles. Coupling this process with low-voltage static electric fields results in a consistent enhancement of the whole deionization treatment, as ions are forced to migrate to the charged electrodes at greater rates. In principle, an electric field can produce a separation of ions even in the absence of the mineral layer; however, the ion removal would be much lower, and flowing water, with multiple passages, would be necessary in order to obtain the target final concentration. In the studied system, the quantity of mineral to be used must be chosen with respect to the amount of water to be treated and to the F^- starting concentration, as adsorption is the only process responsible for the ion removal from water (the number of ions which arrive to the positively charged surface is negligible, and the mineral is supposed to be initially fluoride-free, as was experimentally determined [9]). The possible presence, in the water, of other anions (e.g., Cl^-, CO_3^-, SO_4^{2-}), even in high concentrations, is not expected to significantly modify the electric field intensity (the ion migration rate does not change), and can be faced by just considering the adsorption selectivity and selecting a proper ratio between water and adsorbent: for example, considering the most critical situation simulated here (w_w =20 cm and c_{n0} = 10 mg/L), only 38% of the smectite total adsorption capacity would be necessary to reduce the F^- concentration to 1.5 mg/L. This is sufficient in most real applications according to the literature [49–51]. Considering that the adsorption process is supposed to reach equilibrium conditions, desorption is not possible, even if the voltage application is stopped, since we are considering juvenile waters with approximately constant concentrations in each source. The low voltages tested in this work confirm that the system can be installed and put into operation without using substantial economic resources for the electrical supply, thus representing an appealing opportunity for rural communities of the Ethiopian Rift Valley. Moreover, the device body could be constructed using cheap materials like PVC. Furthermore, the modularity of the system allows an optimum adaptation to the needed quantities of water to be treated and to reasonable processing times.

Future work will consist of testing different adsorption materials and system configurations in order to find better and more efficient solutions.

Author Contributions: Conceptualization, F.F., M.B.L., F.D. and P.V.; methodology, F.F., M.B.L. and F.D.; software, F.F. and M.B.L.; validation, W.G. and P.V.; formal analysis, A.F. and F.D.; investigation, W.G. and P.V.; resources, P.V.; data curation, F.F. and F.D.; writing—original draft preparation, F.F.; writing—review and editing, F.F., M.B.L., W.G., A.F., F.D. and P.V.; visualization, F.D. and P.V.; supervision, F.D. and P.V.; project administration, P.V.; funding acquisition, P.V. All authors have read and agreed to the published version of the manuscript.

Funding: This research was funded by the University of Cagliari (FIR 2020 and DR n° 1044/2009) and Regione Autonoma della Sardegna (GETHERE, grant n. F71/17000190002).

Informed Consent Statement: Not applicable.

Data Availability Statement: The datasets generated for this study are available upon request from the corresponding author.

Conflicts of Interest: The authors declare no conflict of interest. The funders had no role in the design of the study; in the collection, analyses, or interpretation of data; in the writing of the manuscript, or in the decision to publish the results.

References

1. World Health Organization 1 in 3 People Globally Do Not Have Access to Safe Drinking Water—UNICEF, WHO. Available online: https://www.who.int/news/item/18-06-2019-1-in-3-people-globally-do-not-have-access-to-safe-drinking-water-unicef-who (accessed on 2 August 2021).
2. UNICEF; WHO. *The Measurement and Monitoring of Water Supply, Sanitation and Hygiene (WASH) Affordability: A Missing Element of Monitoring of Sustainable Development Goal (SDG) Targets 6.1 and 6.2*; WHO: Geneva, Switzerland, 2021; pp. 1–121.
3. Jagtap, S.; Yenkie, M.K.; Labhsetwar, N.; Rayalu, S. Fluoride in Drinking Water and Defluoridation of Water. *Chem. Rev.* **2012**, *112*, 2454–2466. [CrossRef] [PubMed]
4. Kloos, H.; Tekle Haimanot, R. Distribution of Fluoride and Fluorosis in Ethiopia and Prospects for Control. *Trop. Med. Int. Health* **1999**, *4*, 355–364. [CrossRef]
5. Abiye, T. Groundwater dynamics in the East African rift system. In *Sustainable Groundwater Resources in Africa*; CRC Press: Boca Raton, FL, USA, 2009; pp. 93–106. ISBN 0203859456.
6. Rango, T.; Bianchini, G.; Beccaluva, L.; Tassinari, R. Geochemistry and Water Quality Assessment of Central Main Ethiopian Rift Natural Waters with Emphasis on Source and Occurrence of Fluoride and Arsenic. *J. Afr. Earth Sci.* **2010**, *57*, 479–491. [CrossRef]
7. Ayenew, T. The Distribution and Hydrogeological Controls of Fluoride in the Groundwater of Central Ethiopian Rift and Adjacent Highlands. *Environ. Geol.* **2008**, *54*, 1313–1324. [CrossRef]
8. Tekle-Haimanot, R.; Melaku, Z.; Kloos, H.; Reimann, C.; Fantaye, W.; Zerihun, L.; Bjorvatn, K. The Geographic Distribution of Fluoride in Surface and Groundwater in Ethiopia with an Emphasis on the Rift Valley. *Sci. Total Environ.* **2006**, *367*, 182–190. [CrossRef] [PubMed]
9. Errico, M.; Desogus, F.; Mascia, M.; Tola, G.; Dendena, L. Soil Adsorption Defluoridation of Drinking Water for an Ethiopian Rural Community. *Chem. Pap.* **2006**, *60*, 460–465. [CrossRef]
10. Schulze, D.G. Clay Minerals. In *Encyclopedia of Soils in the Environment*; Elsevier: Amsterdam, The Netherlands, 2005; pp. 246–254.
11. van Olphen, H. A Tentative Method for the Determination of the Base Exchange Capacity of Small Samples of Clay Minerals. *Clay Miner.* **1951**, *1*, 169–170. [CrossRef]
12. Van Olphen, H. Rheological Phenomena of Clay Sols in Connection with the Charge Distribution on the Micelles. *Discuss. Faraday Soc.* **1951**, *11*, 82–84. [CrossRef]
13. Theng, B.K.G.; Russell, M.; Churchman, G.J.; Parfitt, R.L. Surface Properties of Allophane, Halloysite, and Imogolite. *Clays Clay Miner.* **1982**, *30*, 143–149. [CrossRef]
14. Dohrmann, R.; Kaufhold, S.; Lundqvist, B. *Handbook of Clay Science*; Elsevier: Amsterdam, The Netherlands, 2013; Volume 5, ISBN 9780080993645.
15. Huang, H.; Liu, J.; Zhang, P.; Zhang, D.; Gao, F. Investigation on the Simultaneous Removal of Fluoride, Ammonia Nitrogen and Phosphate from Semiconductor Wastewater Using Chemical Precipitation. *Chem. Eng. J.* **2017**, *307*, 696–706. [CrossRef]
16. Siaurusevičiūtė, I.; Albrektienė, R. Removal of Fluorides from Aqueous Solutions Using Exhausted Coffee Grounds and Iron Sludge. *Water (Switz.)* **2021**, *13*, 1512. [CrossRef]
17. Bouhadjar, S.I.; Kopp, H.; Britsch, P.; Deowan, S.A.; Hoinkis, J.; Bundschuh, J. Solar Powered Nanofiltration for Drinking Water Production from Fluoride-Containing Groundwater—A Pilot Study towards Developing a Sustainable and Low-Cost Treatment Plant. *J. Environ. Manag.* **2019**, *231*, 1263–1269. [CrossRef]
18. Owusu-Agyeman, I.; Reinwald, M.; Jeihanipour, A.; Schäfer, A.I. Removal of Fluoride and Natural Organic Matter Removal from Natural Tropical Brackish Waters by Nanofiltration/Reverse Osmosis with Varying Water Chemistry. *Chemosphere* **2019**, *217*, 47–58. [CrossRef] [PubMed]
19. Pan, J.; Zheng, Y.; Ding, J.; Gao, C.; van der Bruggen, B.; Shen, J. Fluoride Removal from Water by Membrane Capacitive Deionization with a Monovalent Anion Selective Membrane. *Ind. Eng. Chem. Res.* **2018**, *57*, 7048–7053. [CrossRef]
20. Aliaskari, M.; Schäfer, A.I. Nitrate, Arsenic and Fluoride Removal by Electrodialysis from Brackish Groundwater. *Water Res.* **2021**, *190*, 116683. [CrossRef] [PubMed]
21. Jiang, K.; Zhou, K.G. Recovery and Removal of Fluoride from Fluorine Industrial Wastewater by Crystallization Process: A Pilot Study. *Clean Technol. Environ. Policy* **2017**, *19*, 2335–2340. [CrossRef]
22. Pillai, P.; Dharaskar, S.; Pandian, S.; Panchal, H. Overview of Fluoride Removal from Water Using Separation Techniques. *Environ. Technol. Innov.* **2021**, *21*, 101246. [CrossRef]
23. Guan, C.; Lv, X.; Han, Z.; Chen, C.; Xu, Z.; Liu, Q. The Adsorption Enhancement of Graphene for Fluorine and Chlorine from Water. *Appl. Surf. Sci.* **2020**, *516*, 146157. [CrossRef]
24. Ruan, Z.; Tian, Y.; Ruan, J.; Cui, G.; Iqbal, K.; Iqbal, A.; Ye, H.; Yang, Z.; Yan, S. Synthesis of Hydroxyapatite/Multi-Walled Carbon Nanotubes for the Removal of Fluoride Ions from Solution. *Appl. Surf. Sci.* **2017**, *412*, 578–590. [CrossRef]
25. He, Y.; Zhang, L.; An, X.; Wan, G.; Zhu, W.; Luo, Y. Enhanced Fluoride Removal from Water by Rare Earth (La and Ce) Modified Alumina: Adsorption Isotherms, Kinetics, Thermodynamics and Mechanism. *Sci. Total Environ.* **2019**, *688*, 184–198. [CrossRef]
26. Liu, J.; Yue, X.; Lu, X.; Guo, Y. Uptake Fluoride from Water by Starch Stabilized Layered Double Hydroxides. *Water* **2018**, *10*, 745. [CrossRef]
27. Borgohain, X.; Boruah, A.; Sarma, G.K.; Rashid, M.H. Rapid and Extremely High Adsorption Performance of Porous MgO Nanostructures for Fluoride Removal from Water. *J. Mol. Liq.* **2020**, *305*, 112799. [CrossRef]

28. Gao, Y.; Li, M.; Ru, Y.; Fu, J. Fluoride Removal from Water by Using Micron Zirconia/Zeolite Molecular Sieve: Characterization and Mechanism. *Groundw. Sustain. Dev.* **2021**, *13*, 100567. [CrossRef]
29. Ghomashi, P.; Charkhi, A.; Kazemeini, M.; Yousefi, T. Removal of Fluoride from Wastewater by Natural and Modified Nano Clinoptilolite Zeolite. *J. Water Environ. Nanotechnol.* **2020**, *5*, 270–282. [CrossRef]
30. Vences-Alvarez, E.; Flores-Arciniega, J.L.; Flores-Zuñiga, H.; Rangel-Mendez, J.R. Fluoride Removal from Water by Ceramic Oxides from Cerium and Manganese Solutions. *J. Mol. Liq.* **2019**, *286*, 110880. [CrossRef]
31. Kim, W.; Singh, R.; Smith, J.A. Modified Crushed Oyster Shells for Fluoride Removal from Water. *Sci. Rep.* **2020**, *10*, 5759. [CrossRef]
32. Mohan, D.; Sharma, R.; Singh, V.K.; Steele, P.; Pittman, C.U. Fluoride Removal from Water Using Bio-Char, a Green Waste, Low-Cost Adsorbent: Equilibrium Uptake and Sorption Dynamics Modeling. *Ind. Eng. Chem. Res.* **2012**, *51*, 900–914. [CrossRef]
33. Bizeray, A.M.; Howey, D.A.; Monroe, C.W. Resolving a Discrepancy in Diffusion Potentials, with a Case Study for Li-Ion Batteries. *J. Electrochem. Soc.* **2016**, *163*, E223–E229. [CrossRef]
34. Kilic, M.S.; Bazant, M.Z.; Ajdari, A. Steric Effects in the Dynamics of Electrolytes at Large Applied Voltages. I. Double-Layer. *Charging. Phys. Rev. E—Stat. Nonlinear Soft Matter Phys.* **2007**, *75*, 021503. [CrossRef]
35. Kilic, M.S.; Bazant, M.Z.; Ajdari, A. Steric Effects in the Dynamics of Electrolytes at Large Applied Voltages. II. Modified Poisson-Nernst-Planck Equations. *Phys. Rev. E—Stat. Nonlinear Soft Matter Phys.* **2007**, *75*, 061909. [CrossRef] [PubMed]
36. Ehlinger, V.M.; Crothers, A.R.; Kusoglu, A.; Weber, A.Z. Modeling Proton-Exchange-Membrane Fuel Cell Performance/Degradation Tradeoffs with Chemical Scavengers. *JPhys Energy* **2020**, *2*, 044006. [CrossRef]
37. Crothers, A.R.; Darling, R.M.; Kushner, D.I.; Perry, M.L.; Weber, A.Z. Theory of Multicomponent Phenomena in Cation-Exchange Membranes: Part III. Transport in Vanadium Redox-Flow-Battery Separators. *J. Electrochem. Soc.* **2020**, *167*, 013549. [CrossRef]
38. Chung, M.H. Numerical Method for Analysis of Tertiary Current Distribution in Unsteady Natural Convection Multi-Ion Electrodeposition. *Electrochim. Acta* **2000**, *45*, 3959–3972. [CrossRef]
39. Chu, K.T.; Bazant, M.Z. Nonlinear Electrochemical Relaxation around Conductors. *Phys. Rev. E—Stat. Nonlinear Soft Matter Phys.* **2006**, *74*, 011591. [CrossRef]
40. Lin, C.; Popov, B.N.; Ploehn, H.J. Modeling the Effects of Electrode Composition and Pore Structure on the Performance of Electrochemical Capacitors. *J. Electrochem. Soc.* **2002**, *149*, A167. [CrossRef]
41. Li, B. Continuum Electrostatics for Ionic Solutions with Non-Uniform Ionic Sizes. *Nonlinearity* **2009**, *22*, 811–833. [CrossRef]
42. Lodi, M.B.; Fanari, F.; Fanti, A.; Desogus, F.; Getaneh, W.; Mazzarella, G.; Valera, P. Preliminary Study and Numerical Investigation of an Electrostatic Unit for the Removal of Fluoride from Thermal Water of Ethiopian Rift Valley. *IEEE J. Multiscale Multiphysics Comput. Tech.* **2020**, *5*, 72–82. [CrossRef]
43. Welch, R.S.; Wilkinson, C.J.; Mauro, J.C.; Bragatto, C.B. Charge Carrier Mobility of Alkali Silicate Glasses Calculated by Molecular Dynamics. *Front. Mater.* **2019**, *6*, 121. [CrossRef]
44. Danilov, D.; Notten, P.H.L. Mathematical Modelling of Ionic Transport in the Electrolyte of Li-Ion Batteries. *Electrochim. Acta* **2008**, *53*, 5569–5578. [CrossRef]
45. Millington, R.J.; Quirk, J.P. Permeability of Porous Solids. *Trans. Faraday Soc.* **1961**, *57*, 1200–1207. [CrossRef]
46. Belhachemi, M.; Addoun, F. Comparative Adsorption Isotherms and Modeling of Methylene Blue onto Activated Carbons. *Appl. Water Sci.* **2011**, *1*, 111–117. [CrossRef]
47. Lu, R.; Leaist, D.G. Mutual Diffusion in Solutions of Alkali Metal Halides: Aqueous LiF, NaF and KF at 25 °C. *J. Chem. Soc. Faraday Trans.* **1998**, *94*, 111–114. [CrossRef]
48. WHO. World Health Organization guidelines for drinking-water quality. In *WHO Chronicle*; WHO: Geneva, Switzerland, 2011; Volume 1, ISBN 978 92 4 154761 1.
49. Mudzielwana, R.; Gitari, M.W. Removal of Fluoride from Groundwater Using MnO_2 Bentonite-Smectite Rich Clay Soils Composite. *Groundw. Sustain. Dev.* **2021**, *14*, 100623. [CrossRef]
50. Zhang, Z.; Tan, Y.; Zhong, M. Defluorination of Wastewater by Calcium Chloride Modified Natural Zeolite. *Desalination* **2011**, *276*, 246–252. [CrossRef]
51. Hamdi, N.; Srasra, E. Removal of Fluoride from Acidic Wastewater by Clay Mineral: Effect of Solid–Liquid Ratios. *Desalination* **2007**, *206*, 238–244. [CrossRef]